

Predicting Subway Passenger Flows under Incident Situation with Causality

Xiannan Huang^a, Shuhan Qiu^a, Quan Yuan^b, Chao Yang^{a,b,*}

^aKey Laboratory of Road and Traffic Engineering, Ministry of Education at Tongji University, 4800 Cao'an Road, Shanghai, 201804, Shanghai, China

^bUrban Mobility Institute, Tongji University, 1239 Siping Road, Shanghai, 200082, Shanghai, China

Abstract

In the context of rail transit operations, real-time passenger flow prediction is essential; however, most models primarily focus on normal conditions, with limited research addressing incident situations. There are several intrinsic challenges associated with prediction during incidents, such as a lack of interpretability and data scarcity. To address these challenges, we propose a two-stage method that separates predictions under normal conditions and the causal effects of incidents. First, a normal prediction model is trained using data from normal situations. Next, the synthetic control method is employed to identify the causal effects of incidents, combined with placebo tests to determine significant levels of these effects. The significant effects are then utilized to train a causal effect prediction model, which can forecast the impact of incidents based on features of the incidents and passenger flows. During the prediction phase, the results from both the normal situation model and the causal effect prediction model are integrated to generate final passenger flow predictions during incidents. Our approach is validated using real-world data, demonstrating improved accuracy. Furthermore, the two-stage methodology enhances interpretability. By analyzing the causal effect prediction model, we can identify key influencing factors related to the effects of incidents and gain insights into their underlying mechanisms. Our work can assist subway system managers in estimating passenger flow affected by incidents and enable them to take proactive measures. Additionally, it can deepen researchers' understanding of the impact of incidents on subway passenger flows.

Keywords: subway incident, passenger flow prediction, causal inference, significant test

1. Introduction

The subway system is a critical component of the transportation network in metropolitan areas due to its environmental benefits, efficiency, and reliability. Understanding passenger flow patterns within these systems is essential for enhancing operational efficiency and user satisfaction. While much research has focused on typical operating conditions, there is a significant gap in addressing unusual situations, such as incidents. Analyzing and predicting how incidents impact passenger flows is vital for subway operators to implement proactive

*Corresponding author, Email: tongjiyc@tongji.edu.cn

strategies. For instance, some studies have concentrated on emergency bus bridging and dispatching models during subway incidents [47, 39], considering the affected passenger numbers as inputs for their models. Consequently, we aim to fill this gap in our paper by proposing a method to **interpret the influence of incident on OD (origination- destination) passenger flows and predict the passenger flows under incident situation**.

There are several papers [54, 26] that focus on predicting passenger flows in subway systems, treating incidents as input features. Since incidents are characteristics of the inputs, these models can predict passenger flows under both normal and incident conditions. They demonstrate improved predictive power and provide valuable insights. However, these models employ complex deep learning methods and end-to-end structures, which obscure the mechanisms by which incidents affect passenger flows. Furthermore, it can be challenging for these models to learn patterns related to incidents in depth, as the number of incidents in subway systems is typically small. Additionally, the imbalance between the volume of data in normal and incident situations may lead the model to prioritize normal conditions, hindering its ability to adequately learn the rules governing incident situations. Finally, the criteria for determining which OD flows are influenced by incidents have not been thoroughly discussed. Some methods [54] assume that the influenced OD flows occur during the incident period and the shortest paths of them include the incident stations. But this assumption is too simple and contradicts reality, for example, even though an incident ends, the effects of it may still persist. And we will elaborate it in the experiment section.

To address these gaps, we propose a two-stage method for predicting passenger flow during incidents, as illustrated in Figure 1. First, a model trained with passenger flow data under normal conditions can be utilized to predict the OD flows that would occur in the absence of an incident. Subsequently, another model can be employed to predict the causal effects of the incident on passenger flows. These causal effects can then be incorporated into the normal OD flow predictions to obtain the final predictions. Besides, these causal effects can also be feed into emergency bus bridging and dispatching models [47, 39] to generate an appropriate bridging bus plan.

This two-stage approach effectively addresses the aforementioned challenges to some extent. For instance, it offers a significant advantage in interpretability: it allows for a detailed analysis of the underlying mechanisms by which incidents impact passenger flows, as the incident model is separated. In contrast, an end-to-end model functions more like a “black box,” making it difficult to analyze the underlying mechanism. Furthermore, in a two-stage framework, high-quality data can be selectively utilized to calibrate the incident model, enhancing its ability to capture incident patterns. This process is more challenging for end-to-end models, as the incident data is often obscured within the normal data. Finally, our method provides flexibility, as each stage can be independently improved. For instance, if a more accurate normal OD prediction model becomes available in the future, it can be directly integrated into the first stage of our method.

In order to complete our prediction method, we will encounter the following four challenges: First, we need to develop an OD prediction model under normal conditions. Second, we must identify the causal effects of incidents on passenger flows using historical data. Third, we need to calibrate a causal effect prediction model based on the identified causal effects. Finally, we must integrate the results from the normal condition prediction model with those from the causal effect prediction model to derive the final predicted OD flows.

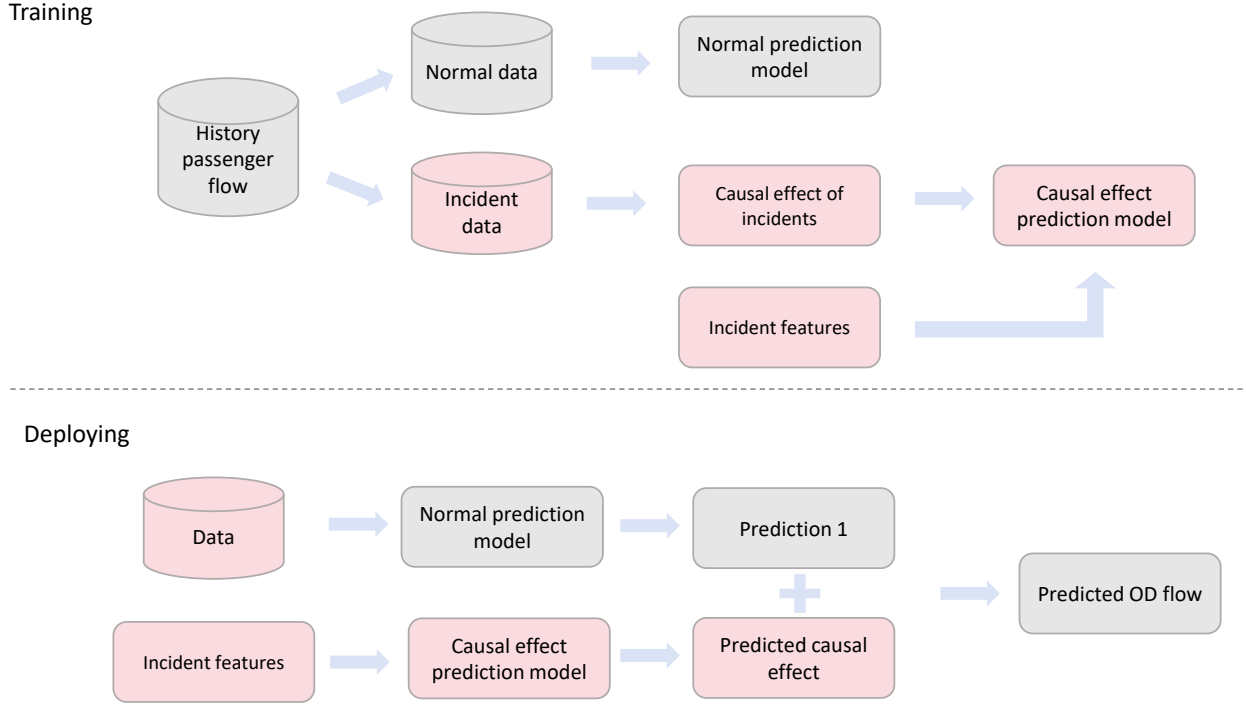


Figure 1: The workflow of our prediction method

While the first challenge is not the primary focus of this paper, we will demonstrate through experiments that any OD prediction model can be utilized in our method, regardless of its specific form. Consequently, the remaining three challenges constitute the main research questions of our study.

To identify the causal effects in historical data, the synthetic control framework is employed to estimate these effects [52]. Besides, to differentiate actual causal effects from noise, placebo tests are utilized to assess the statistical significance of these effects. Furthermore, to calibrate the causal effect prediction model, we examine which types of effects should be used to calibrate the model and propose that only significant effects should be considered. And it is essential to balance both the quantity and quality of data when determining the threshold of significant level. Finally, in the prediction phase, we analyze which types of ODs require correction by the causal effect prediction model and conclude that only significantly affected ODs should be adjusted. Both experimental and theoretical evidence supports the importance of selecting significantly affected ODs for model calibration and passenger flow prediction. We hope our research will provide valuable insights into the patterns of incident effects on passenger flows and offer practical tools for subway station staff to manage incidents effectively. We summarize our contributions as follows:

- We proposed a two-stage OD flow prediction model for subway system under incidents. The first stage is predicting the passenger number under normal situations and the second stage is combining this prediction with the causal effect of incident to obtain the final prediction.
- We used synthetic control method to identify the casual effect from history data and

use placebo test to estimate its significance level.

- We carefully analyzed how to calibrate the causal effect prediction model and how to use it to adjust the results of normal prediction models. The importance of selecting samples that are significantly affected during the calibration and adjustment processes has been proofed both theoretically and experimentally.
- We conducted experiments using real-world data to demonstrate the effectiveness of our method and found some interesting patterns about how incidents affect OD passenger flows.

2. Related Work

2.1. OD passenger flow prediction models

In general, the main challenge of OD prediction is the high dimensionality [53]. For example, if there are 100 stations in a subway system, the number of ODs will be 10000, which could be extremely challenging for traditional models.

To address this, [5, 9] assumed the OD matrix is of low rank and can be reduced to some much smaller matrices. Therefore, some autoregression methods could be employed for these small matrices. And [53] assumed the proportion of passengers of one station to another station compared to the inflow number of this station is a constant, as a result, OD matrix can be directly obtained once the inflow prediction is available. [10] also used station-level embedding to obtain OD matrix and avoid the high dimension problem.

In addition, deep learning method, which is more flexible, expressive and suitable for high dimensional data [15], was used in OD prediction models. For the aspect of time-axis modeling, [40] used LSTM to capture the time information in each time period. [8] employed discrete wavelet transform to capture the fluency information for OD flow in different time periods. And [46] proposed considering day and week periods is important. Besides attention mechanism [12] has been attempted too.

As for spatial information, [6] utilized convolutional neuron network to capture patterns in history OD matrix. [11, 41, 21] attempted graph neuron networks. And [27] used wavelet transform to extract multi-resolution features in OD matrix. [19] introduced dual transformer to capture both temporary and spatial information and predict OD passenger flows. And [10] proposed a module to learn adaptive spatial relationships from data. In summary, even though there are a lot of papers addressing the challenge of OD passenger flow prediction, they often focus on normal conditions and ignore the effects of incidents.

2.2. Evaluating the effects of incident on subway systems

Research about evaluating the effects of incident on subway systems can be broadly categorized into two main areas: network vulnerability or robustness and the impacts of incidents on passenger flows.

2.2.1. Network vulnerability

The majority of studies in this category utilize simulation-based methods or approaches grounded in complex network theory. These methodologies often focus on evaluating network redundancy and robustness. Complex network-based methods conceptualize the subway network as a graph, with stations as nodes and the connections between them as edges. By systematically removing nodes or edges, new graphs are generated, and researchers analyze changes in various coefficients that reflect the network’s structure or passenger travel convenience [7]. This allows for the assessment of incident impacts in different regions and the overall resilience of the subway network.

For instance, [49] analyzed Shanghai’s subway network by removing stations or intervals and evaluating changes in network efficiency, network size, average node centrality, and average edge centrality. This helped determine the vulnerability of specific intervals and assess the network’s overall robustness. Similarly, [48] used changes in network efficiency-related coefficients before and after node and edge deletions to evaluate the vulnerability of subway networks in several cities. Other notable studies include [30, 38]. [51] proposed various indicators to reflect network vulnerability, using concepts from causal inference and actual data to evaluate changes in these indicators under normal and incident scenarios.

Additionally, some research incorporated network passenger flow into models to evaluate the effects of incidents on subway networks [25, 20]. Simulation-based methods were often employed to mimic passenger travel behavior under incident conditions, enabling the evaluation of passenger losses such as increased travel time and congestion costs [29]. And some work considered the cascading failure caused by one incident [28, 34] to evaluate the robustness of subway network, and found the some vulnerable stations or intervals. Furthermore, some articles proposed using simulations to quantify the spillover effects of incidents in specific intervals [45].

2.2.2. Incidents effect on passenger flows

Some studies have utilized passenger flow prediction models to evaluate the effects of incidents. For example, [35] developed a prediction model for subway passenger flow in London based on normal conditions. This model can predict expected passenger flow in the absence of an incident, so this passenger flow can server as a counterfactual value to quantify the impact of subway incident. According to this thought, Other models designed for short-term passenger flow prediction, such as PVGCN [18] and MPSTN [14], could also be adapted to assess the effects of incidents on subway stations.

Besides, [54] created an OD prediction model using smart card data, incorporating incidents as an independent variable. This model can calculate OD values under both incident and non-incident conditions, with the difference indicating the impact of subway incidents on passenger flows. Additional studies have developed specific prediction models for passenger flow during incidents, comparing these results with normal conditions to gauge the impact [42, 43, 24]. Simulation-based approaches have also been used to estimate passenger flow at stations during incidents, thereby evaluating the impact at various stations [44, 36].

Furthermore, [52] utilized real operational data and causal inference methods to assess the effects of subway system disruptions on station passenger flows, highlighting the spillover effects of some disruptions.

Several studies have also analyzed and predicted individual passenger behaviors during

incidents, which can be extended to all passengers and evaluate the change of passenger flow number due to incidents. Some of these works used survey data to understand passenger choices during incidents [32, 22]. Other research leveraged transport card data in consecutive days to identify travel behaviors under incident conditions, and compared these to normal conditions and established predictive models for passenger behavior changes during incidents [37]. Additionally, [23] predicted how many passengers would alter their travel behavior and how these passengers would change their behaviors during incidents.

2.3. Summary

In summary, very few studies address passenger flow prediction for subway systems under incident conditions. And these existing works primarily apply deep learning models, often with simplistic assumptions about which passenger flows are impacted by subway incidents. These studies do not delve into how incidents affect passenger flows in detail, and the interpretability of their models is generally limited.

Moreover, most existing literature about the impact of incidents on subway systems focuses on network vulnerability, often relying on simulations or complex network methods that may not fully reflect real-world subway operations. Besides, their research questions are pretty different compared with the questions proposed in this work. Some studies evaluate the impact of incidents on passenger flow using predictive models, comparing predicted normal conditions with actual passenger flow during incidents. However, these studies lack analysis from causality. Besides, they can only calculate these differences after incidents ended.

3. Method

Our method consists of three parts: causal effect estimation, causal effect prediction model calibration and normal prediction adjustment. We will elaborate them in the following part.

3.1. Causal effect estimation

We have observed that some research focuses on identifying the causal effects of highway incidents on traffic state [16], and they used double robust or inverse propensity weighting methods to address selection biases, i.e., whether an incident happens is related to the influence factors of traffic state. However, incidents in subway systems differ significantly from those on highways, with one of the most notable differences being the number of incidents. The frequency of incidents in subway systems is considerably lower than that in highways. Furthermore, for a specific OD, not all incidents will have an impact on it. Consequently, the number of incidents affecting a specific OD may be even smaller. Therefore, the adjustment of selection biases may be unnecessary. But we require a method to address the issue of having only a limited number of experimental samples.

We use the synthetic control method [2] to calculate counterfactual values and obtain causal effects. This method is widely applied in empirical research within economics and social sciences [1] when only a few samples are intervened. Following the algorithm proposed in [2], we design our approach to estimate the causal effects. But at first, we will give some notations.

Assuming we have a dataset containing n days, with each day divided into m time intervals, let $x_{i,j}$ represent the passenger flow for a specific OD on day i during time interval j . Here, $x_{i,j}^0$ denotes the passenger flow during normal conditions, while $x_{i,j}^1$ indicates the flow after an incident occurs. For simplicity, we assume only one incident occurs in the k -th time interval of day l (our method can be easily generalized to multiple incident situation). Thus, the observed data for a specific OD can be expressed as:

$$\begin{array}{cccccccc}
x_{1,1}^0 & x_{1,2}^0 & \cdots & x_{1,k-1}^0 & x_{1,k}^0 & x_{1,k+1}^0 & \cdots & x_{1,m}^0 \\
x_{2,1}^0 & x_{2,2}^0 & \cdots & x_{2,k-1}^0 & x_{2,k}^0 & x_{2,k+1}^0 & \cdots & x_{2,m}^0 \\
\vdots & \vdots & \ddots & \vdots & \vdots & \vdots & \ddots & \vdots \\
x_{l-1,1}^0 & x_{l-1,2}^0 & \cdots & x_{l-1,k-1}^0 & x_{l-1,k}^0 & x_{l-1,k+1}^0 & \cdots & x_{l-1,m}^0 \\
x_{l,1}^0 & x_{l,2}^0 & \cdots & x_{l,k-1}^0 & \mathbf{x}_{l,k}^1 & \mathbf{x}_{l,k+1}^1 & \cdots & \mathbf{x}_{l,m}^1 \\
x_{l+1,1}^0 & x_{l+1,2}^0 & \cdots & x_{l+1,k-1}^0 & x_{l+1,k}^0 & x_{l+1,k+1}^0 & \cdots & x_{l+1,m}^0 \\
\vdots & \vdots & \ddots & \vdots & \vdots & \vdots & \ddots & \vdots \\
x_{n,1}^0 & x_{n,2}^0 & \cdots & x_{n,k-1}^0 & x_{n,k}^0 & x_{n,k+1}^0 & \cdots & x_{n,m}^0
\end{array} \tag{1}$$

And we want to estimate: $x_{l,k}^1 - x_{l,k}^0$, $x_{l,k+1}^1 - x_{l,k+1}^0, \dots$. It is important to note that $x_{l,k}^1$ is observed, while $x_{l,k}^0$ is not. The latter term represents a **counterfactual value** in the context of causal inference.

Additionally, let $a_{i,j}$ denote the influencing factors for $x_{i,j}$, such as whether day i is rainy, whether it is a weekend, and passenger flow numbers from previous intervals. We assume the dimension of $a_{i,j}$ is d .

The process for synthetic control can be summarized as: **synthetic the unobserved x^0 using observed x^0** , as illustrated in Figure 2, and we will explain this process using the calculation of $x_{l,k}^0$ as an example.

In our setting, $x_{i,k}^0$ is observed for $i \in 1, 2, \dots, l-1, l+1, \dots, n$. We estimate $x_{l,k}^0$ using the following formulation:

$$\hat{x}_{l,k}^0 = \sum_{i \in \{1, 2, \dots, l-1, l+1, \dots, n\}} w_i \times x_{i,k}^0 \tag{2}$$

where each w_i is in $[0, 1]$ and $\sum_i w_i = 1$. This means that if there was no incident on day l , the passenger flow on that day would approximate a weighted-sum of passenger flow numbers on other no-incident days. In other words, we synthesize counterfactual data using observed data, with "synthetic" referring to the weighted sum. For convenience, we use W to signify the vector composed of all w_i 's: $W = (w_1, \dots, w_{l-1}, w_{l+1}, \dots, w_n) \in \mathbb{R}^{n-1}$. The challenge then becomes determining w_i . Recall that a d -dimensional vector $a_{i,j}$ is defined to represent the influence factors of $x_{i,j}$. Therefore, the target of determining W is to make the variable a of the synthetic sample more similar to the a in day l . Let A be the matrix of all $a_{i,j}$'s where $i \in \{1, 2, \dots, l-1, l+1, \dots, n\}$. Thus, $A \in \mathbb{R}^{(n-1) \times d}$. Then W can be determined as:

$$W = \arg \min_W \|a_{l,k} - WA\| = \sqrt{(a_{l,k} - WA)(a_{l,k} - WA)^T} \tag{3}$$

But the importance of each dimension in a may not be equal. As a result, [1] propose to use V -norm instead of l_2 norm and we follow this setting in our method. So W is determined

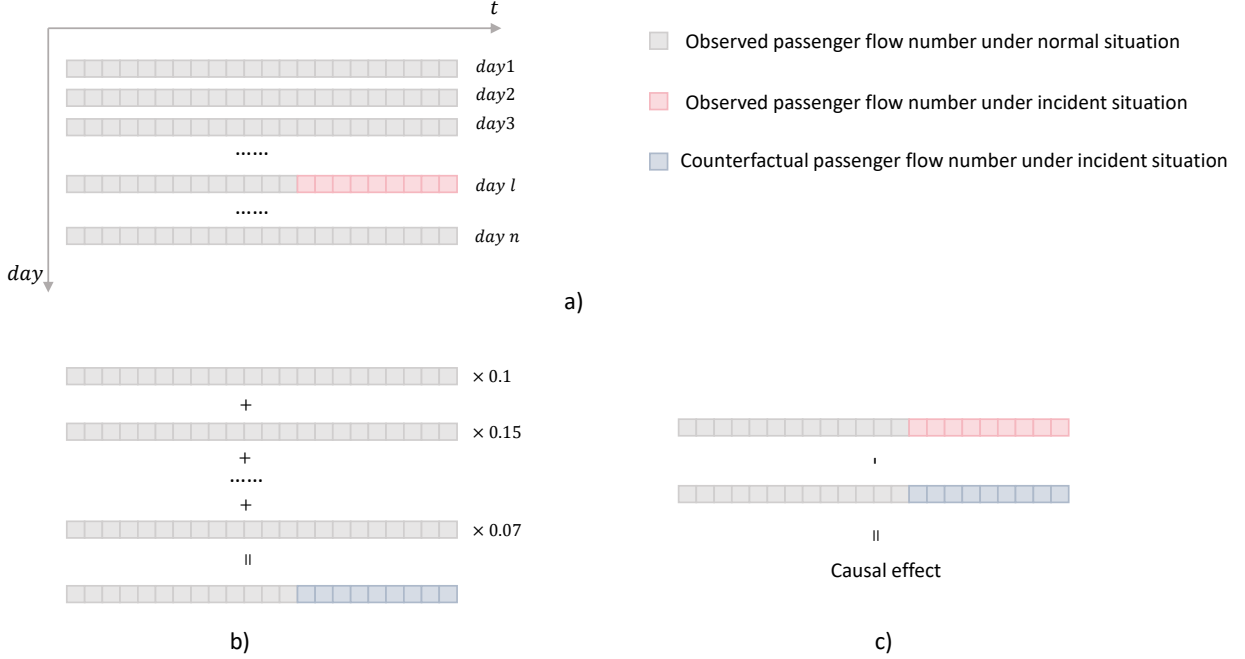


Figure 2: Process of causal effect evaluation: a) Observed data. b) Using observed data in normal cases to synthesize counterfactual data. c) Calculating causal effect.

by:

$$W = \arg \min_W \|a_{l,k} - WA\|_V = \sqrt{(a_{l,k} - WA)V(a_{l,k} - WA)^T} \quad (4)$$

where V is a $d \times d$ positive diagonal matrix. Equation 4 means the influence factors of synthetic counterfactual data, i.e., WA , are similar to the influence factors of actual counterfactual data $a_{l,k}$. The matrix V represents the importance of each dimension in a. According to [1], V can be chosen to minimize the prediction error in previous t time intervals, as the following Equation 5 shows:

$$V = \arg \min_V \|XW(V) - X_0\| \quad (5)$$

where X_0 is a t -dimensional vector, $X_0 = (x_{l,k-t}^0, x_{l,k-t+1}^0, \dots, x_{l,k-1}^0)$, and X is a matrix with shape $t \times (n-1)$, the i -th column of X representing the passenger flow number in time intervals $k-t$ to $k-1$ of day i . $W(V)$ is the function mapping V to W , as defined by Equation 4. For more details, interested readers can refer to [1]. Finally, the causal effect can be estimated as $x_{l,k}^1 - \hat{x}_{l,k}^0$.

Some readers may question that why we do not choose to fit a model form a to x^0 directly but use such a complicated process. This is because directly fitting model could meet the problem of extrapolation and results in inferior performance, this phenomenon has been discussed by [3] and interested readers can refer to it.

3.2. Causal effect prediction model

Even though we can identify the causal effects of incidents on OD flows, these effects are determined only after the incidents have ended and cannot be directly applied to the actual

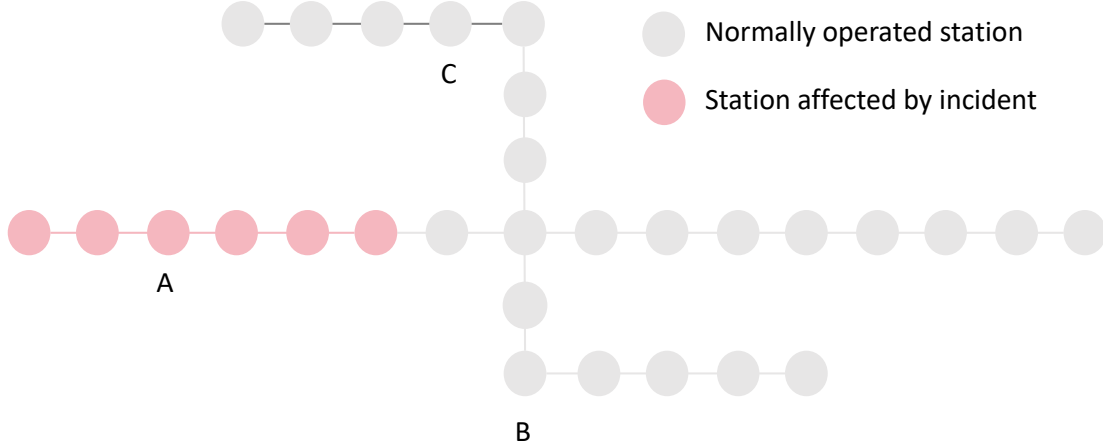


Figure 3: An example of incident

operation of the subway system. Therefore, we need a prediction model to predict the causal effects of incidents on passenger flows immediately after an incident occurs.

3.2.1. Feature selection

First, it is necessary to identify the factors influencing the causal effects. On one hand, the severity of an incident is believed to impact these causal effects. It is reasonable to assume that more severe incidents have a greater potential to affect a larger number of ODs and result in more significant consequences. We have selected six primary indicators to quantify severity: the maximum delay time caused by the incident, the number of trains delayed by five minutes or more, the number of canceled trains, the number of trains that have cleared all passengers, the number of affected stations, and the overall duration of the incident.

On the other hand, the relationship between the ODs and the incident, in both spatial and temporal dimensions, is also considered to influence the causal effects. In the spatial domain, we consider several indicators: the distance from the origin station to the incident interval (where distance is defined as the number of stations on the shortest path, and this definition applies to subsequent distances as well), the distance from the destination station to the incident interval, and the proportion of the shortest path between the origin and destination that overlaps with the incident interval. These indicators reflect the spatial relationship between the ODs and the incident. In the temporal domain, we select the time difference between the OD time and the occurrence of the incident, the time difference between the OD time and the end of the incident, and whether the OD time falls within the duration of the incident. Finally, if the OD originally experiences a higher passenger flow, the causal effect may be more pronounced. Consequently, the counterfactual flow x_0 is also selected.

It is important to note that certain indicators, such as the delay time caused by an incident, the number of trains delayed by five minutes or more and the overall duration of the incident, can only be obtained after the incidents have concluded. Consequently, these indicators cannot be accessed when predicting causal effects. However, we believe this is not a significant issue, as experienced staff in the subway system can generally extrapolate these indicators based on the type or other characteristics of the incident. Additionally,

the severity of the incident must be considered when predicting its causal effects; therefore, we have no choice but to include these indicators. In future work, features related to the types of incidents and the degree of damage to facilities could be considered as indicators of incident severity, and these features can be obtained immediately after an incident occurs. A description of the selected features is provided in Table 1.

Feature	Meaning	Unit
duration	the duration of the incident	minute
max_delay	the delay time caused by the incident	minute
delay_5_num	the number of train trips delayed by five minutes or more	
evacuate_num	the number of trains that required evacuation	
cancel_num	the number of canceled trains	
influence_station_num	the number of stations within the affected interval	
distance_d	the shortest distance from the OD's destination station to the incident interval	
distance_o	the shortest distance from the origin station to the incident interval	
proportion	the proportion of the shortest path between the origin and destination stations that overlaps with the affected interval	
time_diff_to_start	the time difference between the OD time and the incident occurrence time	minute
time_diff_to_end	the time difference between the OD time and the end of the incident	minute
is_in_incident	whether the OD time falls within the incident's duration	
x_0	Predicted counterfactual passenger flow number	

Table 1: Feature Description

3.2.2. Sample selection

According to the formal section, we can calculate the causal effects for all OD pairs and all time intervals for an incident. However, these differences are not solely attributable to the incident; some may be influenced by random effects. For example, an incident situation is show in Figure 3, and this incident may clearly impact the passenger flow from station A to station B, but the effect on the passenger flow from station C to station B may be less apparent. Although the difference between the counterfactual and observed passenger flow from station C to station B can indeed be calculated, it is essential to determine whether this difference is due to random effects or the incident itself. Therefore, it is necessary to select the significantly affected passenger flows, as illustrated in the upper part of Figure 4.

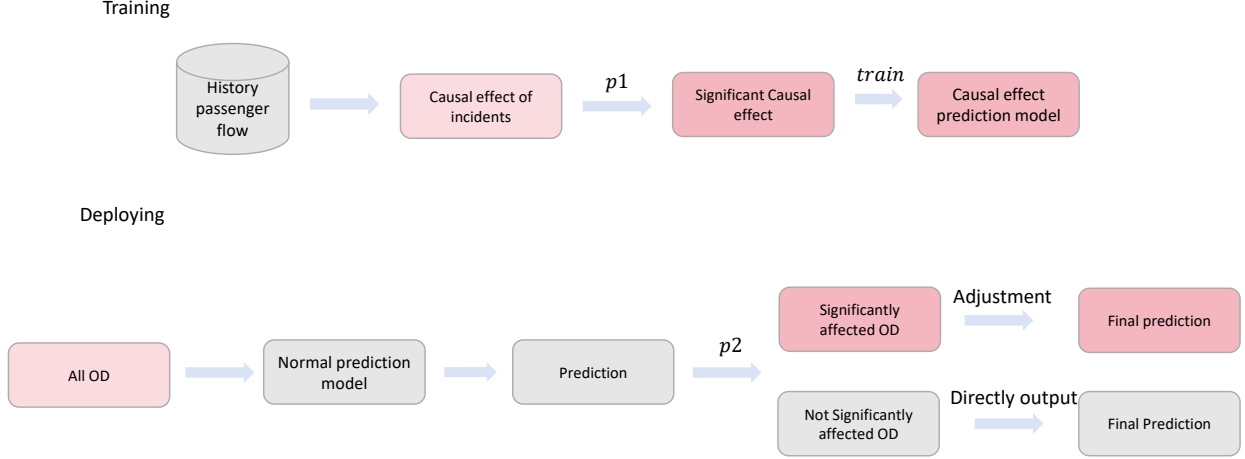


Figure 4: The details of training and deploying causal effect prediction model

We provide a theoretical explanation of why selecting a truly affected sample to calibrate a causal prediction model is important. First, let us consider the following linear model.

Def 3.1. *If the influence factors about the causal effects is noted as x , the causal effect is donated as y , assume y and x obeys the following rule:*

$$y = \epsilon_1 \text{ with probability } 1 - p;$$

$$y = \epsilon_1 + (\beta^T x + \epsilon_2) \text{ with probability } p$$

Where ϵ_1 following normal distribution $N(0, \sigma_1^2)$ and ϵ_2 following normal distribution $N(0, \sigma_2^2)$, β is the parameter and p is a constant between 0 and 1.

This model indicates that in our dataset, only a proportion p of the samples are truly affected samples, while the remaining samples, despite the ability to derive causal effects, are influenced by randomness. Furthermore, the causal effect is a linear function of the influencing factors. We then present a theorem to describe the consequences of fitting a linear model with all samples.

Theo 3.1. *If there are n samples obeying the above model and we directly fit a model with these samples, resulting in the fitted parameter $\hat{\beta}$. Then, the square distance between true parameter and the fitted parameter is:*

$$E(\beta - \hat{\beta})^2 = (1 - p)^2 |\beta|^2 + c \frac{p\sigma_2^2 + \sigma_1^2}{n}$$

Where c is a constant.

It can be founded that the distance is bound by two terms, the first term is $(1 - p) |\beta|^2$, which means the larger the p is, the smaller the loss will be. This law is very intuitive because that if more samples in the dataset are actually affected by incidents, the fitting results will be better. The last term $\frac{p\sigma_2^2 + \sigma_1^2}{n}$ is related to sample size n , which means that the more samples are in the dataset, the better the fitting result will be. This law is also intuitive. In summary, the theorem means that we need to consider both the sample quantity (n) and the sample

quality (p) when selecting which sample should be used to fit the prediction model. As a result, if we just use all OD records after incidents, then the sample quantity n could be large but sample quality p might be small. Therefore, if we can propose a method to judge which causal effect is more likely to be true effect and which is more likely to be randomness, then we can select these true effects and control the sample quality p to be larger and obtain a better fitting result.

Even though we provide only a theoretical analysis of the effect of sample selection on linear models, our experiments indicate that this principle also applies to complex machine learning models.

3.2.3. Significant test

Judging a causal effect is truly because of incident or because of randomness is a classical significant test problem. And we will elaborate it in the following part.

First, our null hypothesis is:

$$H_0 : x_{l,k}^0 = x_{l,k}^1 \quad (6)$$

This null hypothesis means the actual OD flow under incident $x_{i,k}^1$ is the same as the counterfactuals OD flow in normal situation $x_{i,k}^0$. Therefore, the calculated causal effect, i.e., $x_{i,k}^1 - \hat{x}_{i,k}^0$, is because of randomness. We use a placebo test to construct the test statistic [2] and determine whether to reject the null hypothesis. If the null hypothesis is rejected, then we can regard this causal effect is different from zero significantly. The placebo test is widely used, distribution-free and similar to the permutation test. We will elaborate it as follows.

Recall the method from the causal effect estimation section, we use $(a_{i,k}, x_{i,k})$ for $i \in \{1, 2, \dots, l-1, l+1, \dots, n\}$ and $a_{l,k}$ to infer $x_{l,k}^0$. Let f represent this process. Besides, let S denote the set $\{(a_{i,k}, x_{i,k}) \mid i \in \{1, 2, \dots, n\}\}$, and S_{-i} denote the set obtained by removing $(a_{i,k}, x_{i,k})$ from S . Thus, we have:

$$\hat{x}_{l,k}^0 = f(S_{-l}, a_{l,k}) \quad (7)$$

Then we define $e_i = |\hat{x}_{i,k}^0 - x_{i,k}| = |f(S_{-i}, a_{i,k}) - x_{i,k}|$, where $x_{i,k}$ represents the observed passenger flow. Specifically, $x_{i,k} = x_{i,k}^1$ when $i = l$, and $x_{i,k} = x_{i,k}^0$ on other days. Therefore, e_1, e_2, \dots, e_n can be calculated according to our definition.

Intuitively, if the null hypothesis is true, which means $x_{l,k}^0 = x_{l,k}^1$, then all the $(a_{i,k}, x_{i,k})$ follow the same rule since all $x_{i,k}$ equal to $x_{i,k}^0$. Consequently, each error term e_i will follow the same distribution. The order of e_l is equally likely to be in any position from 1 to n . In another word, if e_l is extremely large, for example, the largest among all e_i , it indicates a low probability event happens. Thus, the order of e_l can be viewed as a test statistic to control the type 1 error in the significance test, i.e., to control the significance level.

Let $order(e_l)$ denote the order of e_l among e_1, e_2, \dots, e_n . For example, $order(e_l) = n$ means e_l is the largest element. Then we can use $order(e_l)$ to construct p-value as:

$$p = 1 - \frac{order(e_l)}{n} \quad (8)$$

If the significance level we want to control is α (which is $p1$ in Figure 4) and $p \leq \alpha$, we will reject H_0 and conclude that the incident significantly influenced the passenger flow.

3.3. Prediction adjustment

In practical forecasting tasks, we first utilize a conventional passenger flow prediction model to obtain passenger flow under normal conditions. Subsequently, we utilize a causal effect prediction model to derive the predicted causal effects of specific incident. These causal effects are then used to adjust the passenger flow predictions from the normal model, resulting in passenger flow forecasts under incident conditions. In this section, we concentrate on how to use the causal effect prediction model to correct normal predictions. This approach may seem somewhat peculiar, as one might assume that adjustments could simply be summed together. However, our research underscores the importance of determining which normal predictions should be adjusted.

Taking the example illustrated in Figure 3, it is evident that the passenger flow from station A to station B is likely to be significantly affected by an incident. Therefore, we need to add the causal effect to the predicted passenger flow for the OD from station A to station B. However, the passenger flow from station C to station B raises questions. Should we also adjust the passenger flow for this OD? This remains uncertain, and thus we need to ascertain which passenger flows require adjustment.

We use the following strategy to adjust OD flow prediction: If there are many ODs and these ODs are affected by an incident with different probability according to relationship between these ODs and the incident. Then we note the probability of a specific OD to be affected by the incident is p . Then the strategy is: First determining a threshold P (which is $1 - p^2$ in Figure 4), for each OD, if the probability of the OD to be affected by the incident, i.e., p , is greater than P , we will use causal effect prediction model to adjust it, otherwise we will just regard the prediction of normal model as the final prediction value, as shown in Figure 4. Then we can obtain the risk of this strategy.

Theo 3.2. *If the influence factors about the causal effects is noted as x , the causal effect is donated as y , assume y and x obeys the following rule:*

$$y = \epsilon_1 \text{ with probability } 1 - p$$

$$y = \epsilon_1 + (f(x) + \epsilon_2) \text{ with probability } p$$

Where ϵ_1 following normal distribution $N(0, \sigma_1^2)$ and ϵ_2 following normal distribution $N(0, \sigma_2^2)$, β is the parameter and p is a constant between 0 and 1. If there are a lot of samples (x_i, p_i) and a prediction model

$$\hat{y} = \hat{f}(x)$$

Then we can get the risk of the above strategy.

$$E(y - \hat{y})^2 = \frac{1}{2}P^2(Ef(x)^2 + E\hat{f}(x)^2 - E(\hat{f}(x) - f(x))^2) - PE\hat{f}(x)^2 + c$$

Where c is a constant. and the expectation is taken over x and ϵ_1, ϵ_2 .

The risk is a quadratic function of P , then to obtain the minimum risk, we should set P as:

$$P = \frac{E\hat{f}(x)^2}{Ef(x)^2 + E\hat{f}(x)^2 - E(f(x) - \hat{f}(x))^2} \quad (9)$$

Some detailed analysis of this theorem is given as follows. First, when $\hat{f}(x) = f(x)$, which means the causal effect prediction model is completely correct, then we have $P = 1/2$. This strategy means that if we know the probability for an OD to be affected by an incident is great than 0.5, we will use the causal effect prediction model to adjust this OD passenger flow, otherwise, we will not adjust it. Besides, when $E\left(f(x) - \hat{f}(x)\right)^2$ is smaller, in other words, the mean square error of causal effect prediction model is smaller, the best P could be smaller. This rule means more samples can be adjusted if the model is more accurate and it also conforms intuition. Finally, when the magnitude of causal effect, i.e. $E f(x)^2$, is greater, the P should be set to a smaller value, which means more samples should be adjusted.

Besides, the probability of a specific OD to be affected by the incident, i.e., p_i , is not known, but we can use the p-value in history data (calculated by significant test section) and some influence factors to fit a model to predict p . As a result, the workflow of training and deploying the causal effect prediction model could be shown in Figure 4, and $p1, p2$ in the figure are thresholds used to select training samples and samples need correction.

4. Experiments

4.1. Data description

The data utilized in our study is derived from the Shanghai subway system, one of the largest and most complex subway networks in China, which comprises 20 lines and 508 stations.

The first part comprises OD data from the Shanghai subway system. The timing of ODs is determined by the exit time, with a temporal granularity of thirty minutes. The data covers the period from January 1, 2024, to March 24, 2024. We excluded data from the New Year’s holiday and the Chinese New Year period because their unique passenger flow patterns differ significantly from those of regular weekdays.

The second part of our dataset includes incident records from the Shanghai subway system. These records provide a detailed description of each incident, including the start time, end time, maximum delay caused by the incident, the number of canceled trains, and other relevant information.

Most incidents in our dataset had minimal impact, resulting in no or insignificant delays. Consequently, we only selected those incidents that caused delays exceeding five minutes. Additionally, we excluded incidents that occurred during the early morning hours, such as those involving the first train of the day, as passenger flow during these times is inherently low, rendering the analysis less meaningful. Ultimately, we identified six eligible incidents, with the last incident in our dataset occurring on March 14th. Our objective is to utilize the data prior to March 14th to build models that predict passenger flow on that day. It is noted that the incident began at 7:15 a.m. and ended at 9:24 a.m.; therefore, our focus is to predict passenger flows between 7:00 a.m. and 12:30 a.m. Given that the incident occurred in suburban sections, OD pairs whose origin and destination stations are not located on the incident line are unlikely to be affected. Therefore, our analysis concentrates on ODs with at least one station (either the origin or destination) located on the incident line.

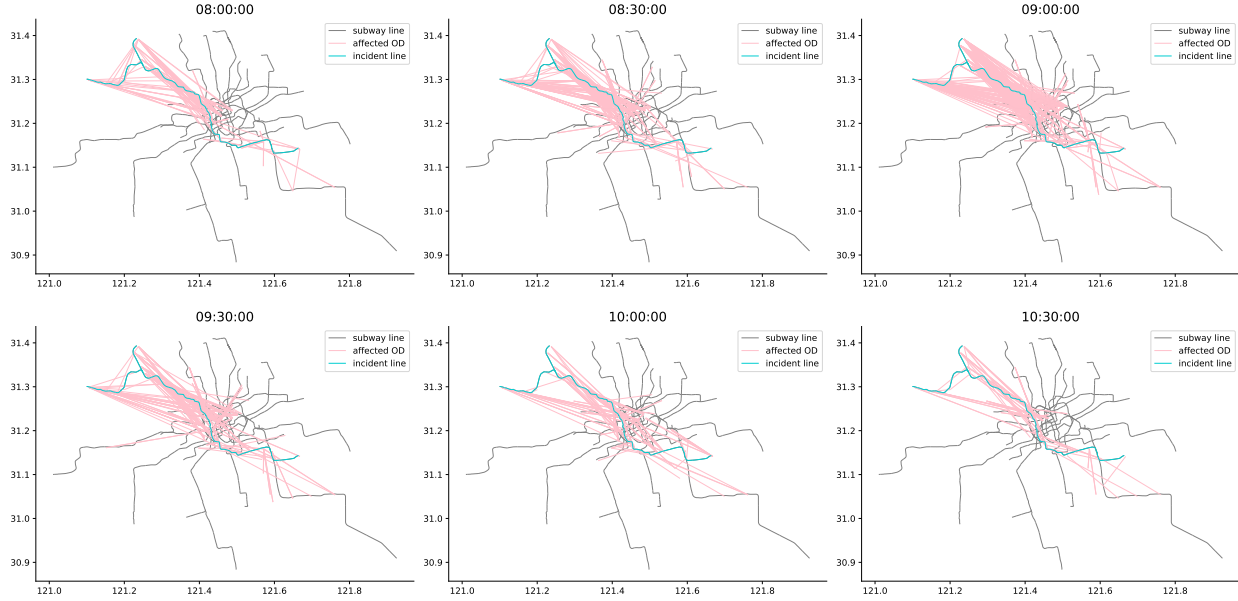


Figure 5: Significantly influenced ODs in different time intervals

4.2. Causal effect identification results

The details in causal effect identification are first explained. As previously mentioned in Equation 4 of Method section, we need to consider several influencing factors a for an OD. In this paper, we use weather conditions (whether it is sunny), whether it is a weekend, and historical passenger flow volume from the previous two time periods as a . Similarly, when we determine V using Equation 5, we also rely on historical data from the previous two time periods to construct X_0 and X . The significance level used in our analysis is 0.05.

The effect of an incident typically increases with its onset and gradually dissipates as the incident ends. Consequently, we analyze all OD pairs from the beginning of an incident until three hours after its end. Using the model proposed in the Method section, we identify the causal effects of each subway incident and conduct significance tests on these effects. However, due to space limitations, we only provide a detailed report on the causal effect identification results for the incident in 11th Marth. The details of this incident are as follows:

Starting at 7:45 on the 11th Marth, a vehicle malfunction occurred on Line 11, and the malfunctioning vehicle was arranged to proceed slowly. From 7:51 to 8:43, temporary passenger flow control measures were implemented at Malu, Chenxiang Highway, Nanxiang, Taopu Xincun, Qilianshan Road, Liziyuan, and Fengqiao Road stations.

Figure 5 illustrates the significantly affected ODs identified during the six time periods from 8:00 AM to 10:30 AM. In the figure, the blue line represents the subway line where the incident occurred, the black lines denote regular subway lines, and the red lines indicate the ODs that were significantly impacted by the incident.

It should be noted that the incident occurred at 7:45 AM and ended at approximately 8:45 AM. As illustrated in Figure 5, the number of affected ODs initially increased and peaked between 8:30 and 9:00 AM, before gradually declining. By 10:00 and 10:30 AM, only

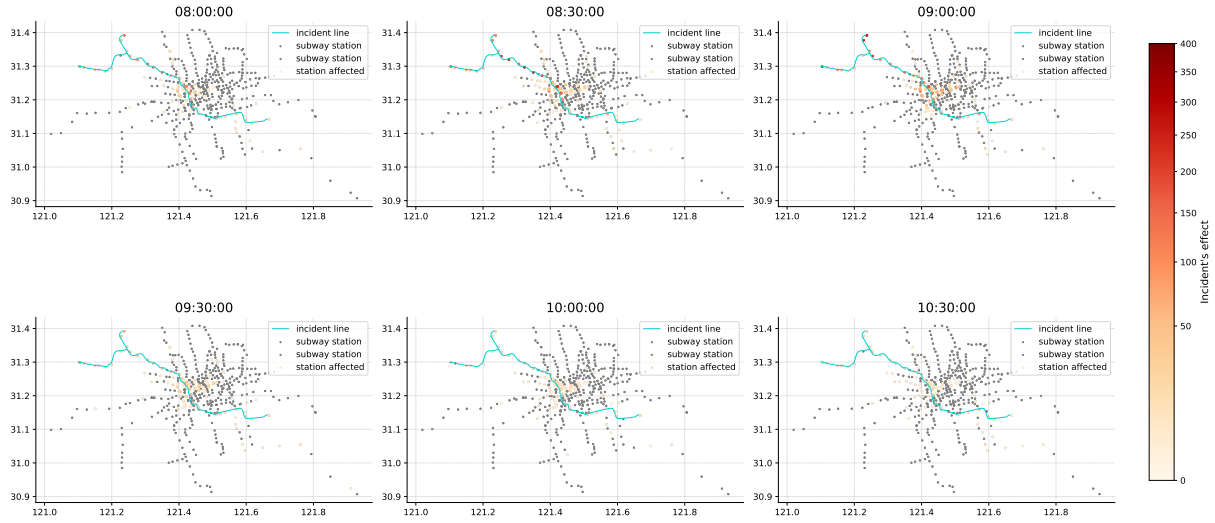


Figure 6: Incident's effects on stations in different time

a few ODs remained affected. Additionally, at the onset of the incident, relatively few ODs were impacted, as the effects had not yet spread widely.

Furthermore, the affected stations are primarily located in the northern part of Shanghai. Figure ?? confirms that the ODs affected by this incident are predominantly situated in the northern region, which is consistent with the actual situation.

Besides, Figure 6 illustrates the stations affected over various time periods and the corresponding levels of impact. The impact level of each station is determined by summing the absolute values of causal effects across all ODs related to this station. Black points represent unaffected stations, while the colors of affected stations range from yellow to red, with redder points indicating higher levels of impact. The blue line denotes the incident subway route. It can be concluded that between 8:00 and 9:00, a greater number of stations were affected, exhibiting stronger impacts. As time progressed, both the number of affected stations and the levels of impact decreased.

For further analysis, four significantly affected ODs are selected: Jiading West to Chenxiang Road, Jiangsu Road to Jing'an Temple, Xujiahui to Dapu Bridge, and Jiading North to Nanxiang. The passenger flow numbers for these four ODs over an eight-day period, from March 11th to March 20th are illustrated in Figure 7.

First, it is important to note that March 11th is a Monday, and the following Monday is March 18th. Additionally, there is no data for March 16th due to missing data in the original dataset. Each subplot in Figure 7 illustrates the changing trend of an OD, with the gray box on March 11th indicating the time of the incident.

For these four ODs, the patterns observed during the incident period differ significantly from those on other days. For example, the top subplot, which illustrates the OD from Jiading West to Chenxiang Road, indicates that the OD value within the gray box is considerably higher compared to other weekdays, such as March 12th, March 13th, and the

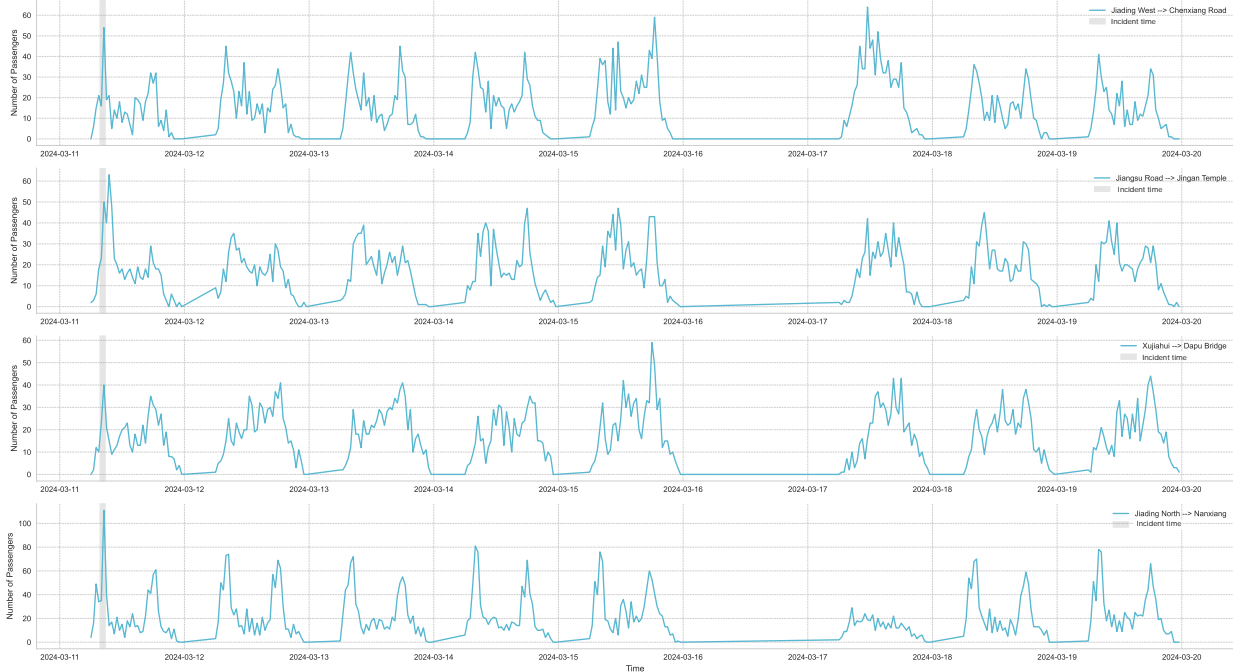


Figure 7: Passenger flow numbers of four significantly influenced ODs

following Monday, March 18th. Similar patterns can be observed in the other three ODs. This phenomenon may be attributed to the primary consequence of the incident: delays occurring around 8:00 AM. These delays could lead passengers who would typically take the subway at 8:00 AM to board later, while those who planned to travel after 8:00 AM continued with their original schedules. This overlap of passengers resulted in a heightened peak during the morning rush hour.

4.3. Passenger flow prediction results

In this section, we conducted experiments to determine whether the proposed two-stage approach enhances the accuracy of passenger flow predictions under incident conditions. We began by selecting baseline prediction models under normal situations. These models include three traditional machine learning algorithms: Linear Regression (LR), Random Forest (RF), and Gradient Boosted Decision Trees (GBDT).

We selected two matrix-based models: ST-ResNet [50] and UNet [31], which are widely utilized for matrix data, and GEML [41], a model specifically designed for Ride-hailing OD prediction.

We also conducted experiments with different causal effect prediction models. Specifically, we selected three models: Linear Regression, Random Forest, and Gradient Boosted Decision Trees. Following [54], we omitted the ODs with passenger flow less than 2. Besides, MAE (mean absolute err), RMSE (root mean square error) and MAPE (mean absolute percentage error) are used to evaluate the prediction accuracy. The equations to calculate them are in follows.

$$MAE = \frac{1}{n} \sum |\hat{y} - y|$$

$$RMSE = \sqrt{\frac{\sum (\hat{y} - y)^2}{n}}$$
$$MAPE = \frac{1}{n} \sum \frac{|\hat{y} - y|}{y}$$

Where \hat{y}, y are the true and predicted OD flows, and n is the total number OD flows. The results of experiments are reported in Table 2.

Normal prediction model	Causal effect prediction model	Original model						Two stage model						Improvement	
		All OD			Influenced OD			All OD			Influenced OD			All OD	Influenced OD
		MAE	RMSE	MAPE	MAE	RMSE	MAPE	MAE	RMSE	MAPE	MAE	RMSE	MAPE		
LR	LR	2.177	3.344	14.6%	6.662	7.851	35.9%	2.058	3.139	13.6%	4.888	6.474	30.4%	5.5%	26.6%
	RF							2.017	3.005	13.1%	4.515	5.971	28.4%	7.4%	32.2%
	GBDT							2.037	3.045	13.3%	4.658	6.093	29.5%	6.4%	30.1%
RF	LR	1.902	2.771	12.5%	5.817	7.295	28.1%	1.820	2.781	12.8%	4.478	5.916	28.7%	4.3%	23.0%
	RF							1.784	2.650	12.4%	3.882	5.194	25.6%	6.2%	33.3%
	GBDT							1.807	2.737	12.9%	4.355	5.733	29.2%	5.0%	25.1%
GBDT	LR	1.909	2.790	12.1%	5.869	7.378	27.6%	1.824	2.897	13.1%	4.427	5.315	27.9%	4.5%	24.6%
	RF							1.779	2.646	12.8%	3.995	5.302	26.5%	6.8%	31.9%
	GBDT							1.808	2.743	12.8%	4.368	5.760	27.7%	5.3%	25.6%
ST-ResNet	LR	1.872	2.703	10.5%	6.313	7.525	29.2%	1.794	2.605	12.3%	4.169	5.493	26.9%	4.1%	34.0%
	RF							1.761	2.573	12.2%	4.118	5.418	26.6%	5.9%	34.8%
	GBDT							1.777	2.583	12.3%	4.152	5.463	26.7%	5.1%	34.2%
U-Net	LR	1.848	2.594	10.4%	6.274	7.689	31.2%	1.787	2.702	12.4%	4.287	5.673	27.7%	3.3%	31.7%
	RF							1.730	2.605	12.3%	4.169	5.493	26.9%	6.4%	33.6%
	GBDT							1.741	2.663	12.4%	4.236	5.568	27.3%	5.8%	32.5%
GEML	LR	1.895	2.644	9.9%	6.205	7.591	29.8%	1.829	2.710	12.5%	4.270	5.598	27.5%	3.5%	31.2%
	RF							1.789	2.654	12.4%	4.236	5.568	27.3%	5.6%	31.7%
	GBDT							1.797	2.637	12.4%	4.220	5.538	27.1%	5.1%	32.0%

Table 2: Experiment results

First, we summarize the performance of these baseline models without adjustments for causal effects. The errors on all passenger flows and significantly affected passenger flows (p-values ≤ 0.05) show that most models meet a substantial increase in error when predicting the flows of significantly affected ODs. In these cases, errors even surge by as much as three times. Traditional machine learning methods generally produce higher prediction errors across all flows compared to deep learning models. However, for significantly affected flows, traditional models exhibit lower prediction errors than deep learning models. This discrepancy may arise because deep learning models capture subtle and sensitive data patterns that may not be applicable under incident conditions, resulting in rapid increases in error when deployed in such scenarios.

Table 2 demonstrates that our two-stage method—first predicting with traditional models and then adjusting based on causal effects—significantly enhances accuracy, particularly for passenger flows that are significantly impacted. For overall passenger flows, we observe error reductions of approximately 4-7%. In the case of incident-affected flows, error reductions reach 20-30%. These findings validate the effectiveness of our approach.

Moreover, the results presented in Table 2 indicate that the Random Forest algorithm yields the most accurate predictions of causal effects, followed by Gradient Boosted Decision Trees, while Linear Regression offers the least improvement. This finding aligns with intuitive reasoning, as the impact of incidents on subway passenger flow is likely non-linear and may involve complex interactions. These mechanisms will be discussed in greater detail in the following section

4.4. Analysis of causal effect prediction model

In this section, we aim to answer a key question: how do these selected features influence the causal effects of incidents? Given that the Random Forest model demonstrated superior predictive accuracy, we conducted an in-depth analysis of the Random Forest model. First, we determine the importance of each feature in the Random Forest model, as shown in Table 3.

Feature	Importance
x_0	0.493
time_diff_to_start	0.116
time_diff_to_end	0.076
proportion	0.068
max_delay	0.056
distance_o	0.041
distance_d	0.034
duration	0.015
cancel_num	0.013
delay_5_num	0.012
is_in_incident	0.010
clear_num	0.008

Table 3: Feature importance

Table 3 shows that the counterfactual passenger flow (x_0) is the most significant element affecting the causal effect of incidents, which is consistent with common sense. This demonstrates that if an OD has a higher baseline passenger flow, an incident will have a greater influence on that flow. In contrast, for OD with smaller baseline flows, the incident exhibits a modest effect it. Other key factors include the time from the start and end of the incident to the time of OD, which also corresponds to common expectations. If the interval is too short, there may not be sufficient time for the incident to influence passenger flow; if it is too long, the impact might have already dissipated. Therefore, the time interval is crucial to the effect of the incident. Additionally, the delay duration caused by the incident is also highly important, which makes sense, as longer delays generally reflect more severe incidents, and therefore, a greater impact on passenger flow. However, features such as the number of canceled trains and the number of five-minute delay trains appear less significant. This might be because the severity of incidents does not directly correspond to these metrics. For instance, the count of five-minute delay trains might increase as the incident becomes more serious, but as the severity intensifies further, some delayed trains might be canceled, causing the number to drop. The lack of a one-to-one relationship suggests that this metric may not clearly reflect the severity of incidents. These findings indicate that future models may benefit from including indicators that reflect the incident severity more accurately.

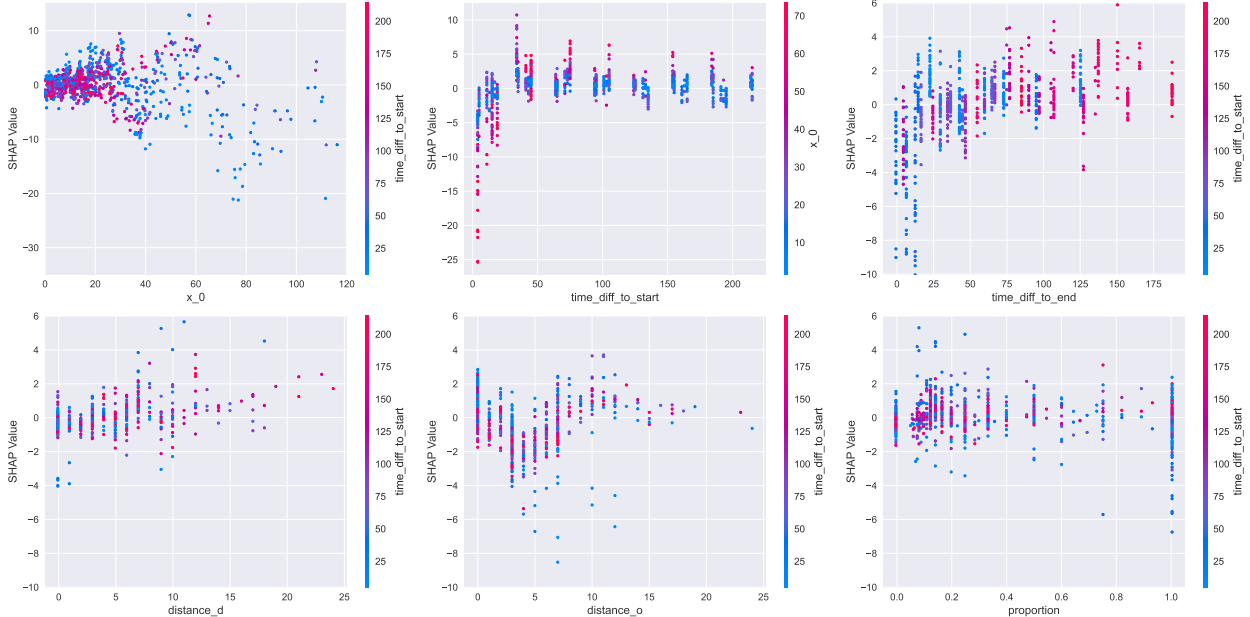


Figure 8: Partial dependence plots for some features

Moreover, we analyzed model outputs by plotting partial dependence plots (PDPs) using the SHAP method [33]. Each subplot in Figure 8 represents a PDP and shows the interaction between two variables, where the x-axis indicates one variable and the color represents another. For example, in the first subplot, larger counterfactual baseline flows (x_0) generally correlate with stronger causal effects. However, the signs of the causal effect vary by color, which reflects the time difference between the OD and the start of the incident. Smaller differences (bluer points) tend to have negative causal effects, indicating suppressed flow,

while larger differences (redder points) suggest increased flow, as some users delay travel and lead to a recovery effect.

Similar patterns appear in the second subplot in the first row, where causal effects are predominantly negative when time differences are below 30 min, turning positive at around 50-100 minutes, possibly indicating flow recovery. After 100 minutes, causal effects diminish around zero, and negative effects tend to be stronger than positive ones. This implies that a subway incident could lead to an initial sharp drop in passenger flow, followed by gradual recovery. Even after the incident ends, the flow may remain slightly above the normal levels.

The first and second subfigures in the second row illustrate how the distance from the incident location to the origin and destination stations affects the causal effects. The effect is generally stronger when the distance is within approximately 10, but it diminishes significantly beyond this range. When the distance is less than 10, the absolute values of the causal effect are relatively consistent, suggesting a threshold effect of distance. Additionally, the distance to the origin station has a more pronounced influence on the causal effect than the distance to the destination station.

4.5. Validation of sample selection

In the method section, we proposed that it is important to select samples that are significantly impacted to calibrate causal effect prediction model. In deployment, choosing passenger flows which are significantly affected by incidents is also beneficial. To validate this statement, and to analyze how different threshold values ($p1$ and $p2$ in Figure 4) affect overall prediction error, we conducted further analysis.

Specifically, we used Random Forest as the baseline model under normal situation. First, we fixed $p1$ at 0.05 and adjusted $p2$ to observe how changes in $p2$ impact overall prediction error. We examined three causal effect prediction models: Linear Regression, Random Forest, and Gradient Boosted Decision Trees, producing the three subplots in the lower half of Figure 9.

Next, we fixed $p2$ at 0.05 and adjusted $p1$, varying it between 0 and 1. For each setting, we repeated the model calibration and deployment processes, measuring the final overall passenger flow prediction accuracy. We again used Linear Regression, Random Forest, and Gradient Boosted Decision Trees as causal effect prediction model, respectively. The results are shown in the top three subplots in Figure 9.

From the top three subplots in Figure 9, we observe that prediction error is high when $p1$ is set either very low (close to zero) or very high (close to one). The lowest prediction errors occur when $p1$ is in the middle range, around 0.03 to 0.08, which aligns with previous theoretical expectations. Comparing the three prediction models, we see that Linear Regression achieves optimal prediction accuracy with a smaller $p1$ value, around 0.03, while Random Forest and Gradient Boosted Decision Trees require a slightly larger $p1$.

This finding aligns with prior analysis: the final prediction error is determined by both the quantity and quality of selected samples. For the linear model, which has fewer parameters compared to tree-based models, fewer samples are needed to achieve adequate calibration. This allows for a smaller threshold ($p1$), ensuring higher-quality samples are selected.

Observing the lower half of Figure 9, it can be found that when $p2$ is either too low, such as zero, or too high, close to one, the prediction error of the model is relatively large. Only when $p2$ falls within a reasonable range, approximately 0.1, does the model achieve optimal

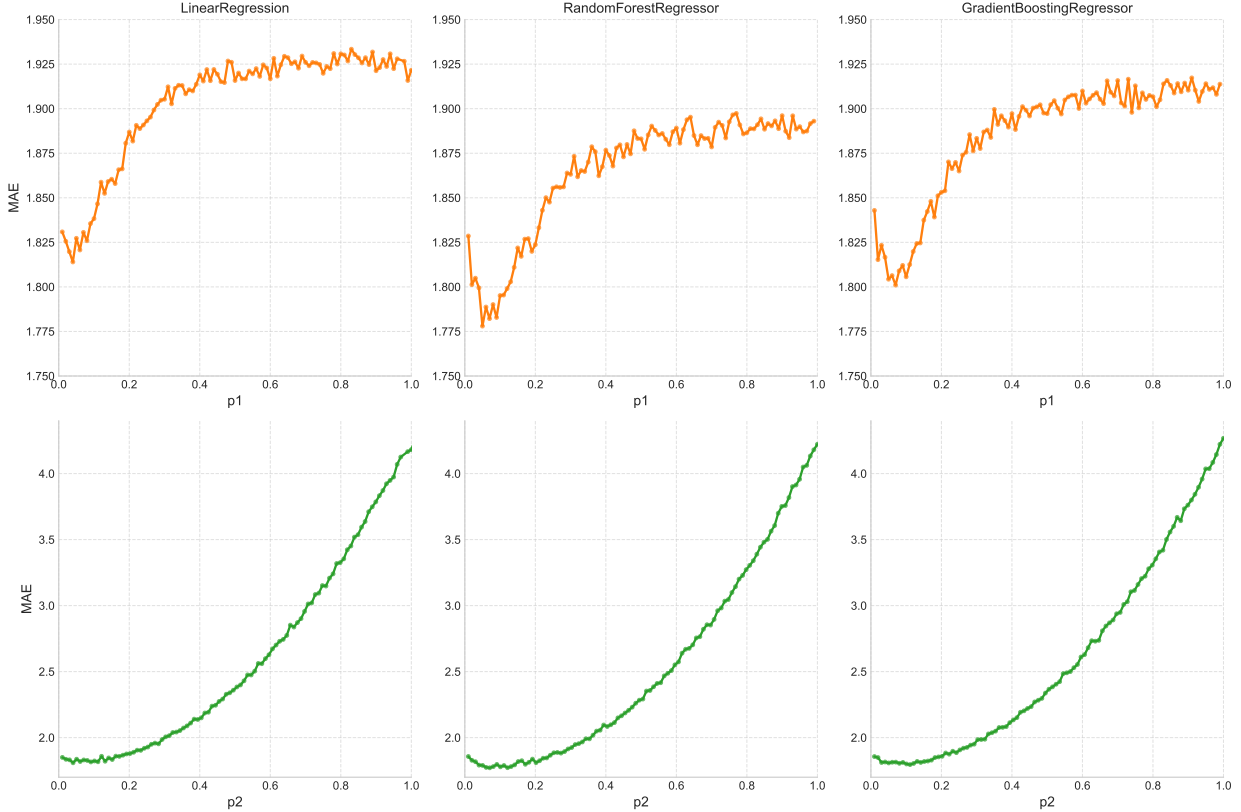


Figure 9: The relation between p_1, p_2 and prediction errors

prediction accuracy. Additionally, the relationship between p_2 and the final prediction error resembles a quadratic function, which aligns well with the result of Theorem 3.2. This similarity supports the validity of our theoretical findings.

A cross-model comparison also reveals that the optimal p_2 value for Linear Regression is smaller compared to the other two models. This observation is consistent with previous analysis, which suggests that models with higher goodness of fit in causal effect prediction need a larger p_2 threshold. Complex tree-based models, such as Random Forest and Gradient Boosted Decision Trees, exhibit better fit than Linear Regression, allowing them to adopt higher p_2 values for sample selection.

5. Conclusion

In this paper, we propose a two-stage method to predict subway passenger flows under incident conditions. In the training phase, we first use synthetic control methods to evaluate the causal effects of incidents on passenger flows, followed by calibrating a model using incident and passenger flow features to predict these causal effects. And a prediction model for normal situation is trained. In the deployment phase, the normal model predicts passenger flows without incidents. Then, the causal effect prediction model is used to estimate the effects of the incident, and the two results are combined to obtain the final prediction. We also use placebo test method to obtain the significant level of causal effect and the importance

of it is validated both theoretically and experimentally. The experimental results based on real-world data demonstrate the effectiveness of the proposed method.

The two-stage style provides advantages in interpretability and flexibility. In terms of interpretability, the model allows for an analysis of incident’s effects, identifying how the impact of incidents spreads and dissipates, and how passenger flows are suppressed and then gradually recover. In terms of flexibility, different models can be used for normal flow prediction and causal effect prediction, with the potential for improved accuracy using more advanced models in the future.

There are several limitations in our current work which could be improved. First, our dataset is relatively small, covering only three months and six serious incidents. This limited sample size may affect the model’s robustness, suggesting the need for a larger dataset in future studies.

Second, the current causal identification and causal effect prediction models rely on traditional methods, without accounting for potential spatial relationships in causal effects. In the future, spatial information could be used to estimate causal effects more accurately. For instance, in estimating counterfactual passenger flow through synthetic control methods, it might be helpful to incorporate spatially related flows to decide weights W in Eq3. Additionally, traditional models, such as Random Forest and linear regression, are used as causal effect prediction models in this research. In the future, using deep spatial-temporal neural networks might lead to improvements. Moreover, incorporating more features, such as bus schedules and land usage, may improve the prediction results.

Finally, forecasting passenger flow under special conditions remains challenging due to limited data on such scenarios. When collecting sufficient data proves difficult, large language models (LLMs) could offer an alternative, as recent research has shown that LLMs, with their extensive world knowledge and generalization ability, can make reasonable predictions for unusual scenarios [13, 17]. Integrating LLMs for subway passenger flow prediction under incident conditions may be a promising future direction.

In summary, our work can help subway operators predict changes in passenger flow after incidents, providing input for designing alternative transportation or implementing emergency measures. It can also deepen researchers’ understanding of the mechanisms behind the effects of incidents on passenger flows.

References

- [1] Abadie, A., 2021. Using synthetic controls: Feasibility, data requirements, and methodological aspects. *Journal of Economic Literature* .
- [2] Abadie, A., Diamond, A., Hainmueller, J., 2010. Synthetic control methods for comparative case studies: Estimating the effect of california’s tobacco control program. *Journal of the American Statistical Association* 105, 493 – 505.
- [3] Abadie, A., Diamond, A., Hainmueller, J., 2014. Comparative politics and the synthetic control method. *ERN: Estimation (Topic)* .
- [4] Bilodeau, M., Brenner, D., 1999. *Theory of multivariate statistics*. Springer Science & Business Media.

- [5] Cheng, Z., Trépanier, M., Sun, L., 2021. Real-time forecasting of metro origin-destination matrices with high-order weighted dynamic mode decomposition. *Transp. Sci.* 56, 904–918.
- [6] Chu, K.F., Lam, A.Y.S., Li, V.O.K., 2020. Deep multi-scale convolutional lstm network for travel demand and origin-destination predictions. *IEEE Transactions on Intelligent Transportation Systems* 21, 3219–3232.
- [7] Derrible, S., Kennedy, C.A., 2010. The complexity and robustness of metro networks. *Physica A-statistical Mechanics and Its Applications* 389, 3678–3691.
- [8] Diao, Z., Zhang, D., Wang, X., Xie, K., He, S., Lu, X., Li, Y., 2019. A hybrid model for short-term traffic volume prediction in massive transportation systems. *IEEE Transactions on Intelligent Transportation Systems* 20, 935–946. doi:10.1109/TITS.2018.2841800.
- [9] Gong, Y., Li, Z., Zhang, J., Liu, W., Zheng, Y., 2020. Online spatio-temporal crowd flow distribution prediction for complex metro system. *IEEE Transactions on Knowledge and Data Engineering* 34, 865–880.
- [10] Han, L., Ma, X., Sun, L., Du, B., Fu, Y., Lv, W., Xiong, H., 2022. Continuous-time and multi-level graph representation learning for origin-destination demand prediction. *Proceedings of the 28th ACM SIGKDD Conference on Knowledge Discovery and Data Mining* .
- [11] Hu, J., Yang, B., Guo, C., Jensen, C.S., Xiong, H., 2020. Stochastic origin-destination matrix forecasting using dual-stage graph convolutional, recurrent neural networks, in: 2020 IEEE 36th International Conference on Data Engineering (ICDE), pp. 1417–1428. doi:10.1109/ICDE48307.2020.00126.
- [12] Huang, B., Ruan, K., Yu, W., Xiao, J., Xie, R., Huang, J., 2023. Odformer: Spatial-temporal transformers for long sequence origin-destination matrix forecasting against cross application scenario. *Expert Systems with Applications* 222, 119835. URL: <https://www.sciencedirect.com/science/article/pii/S0957417423003366>, doi:<https://doi.org/10.1016/j.eswa.2023.119835>.
- [13] Huang, X., 2024. Enhancing traffic prediction with textual data using large language models. *ArXiv abs/2405.06719*.
- [14] Huang, X., Yang, C., Yuan, Q., . Leveraging intra-period and inter-period features for enhanced passenger flow prediction of subway stations, in: 103rd Annual Meeting of the Transportation Research Board. doi:10.48550/arXiv.2410.14727.
- [15] LeCun, Y., Bengio, Y., Hinton, G., . Deep learning 521, 436–444. URL: <https://doi.org/10.1038/nature14539>, doi:10.1038/nature14539.

- [16] Li, S., Pu, Z., Cui, Z., Lee, S., Guo, X., Ngoduy, D., . Inferring heterogeneous treatment effects of crashes on highway traffic: A doubly robust causal machine learning approach 160, 104537. URL: <https://linkinghub.elsevier.com/retrieve/pii/S0968090X24000585>, doi:10.1016/j.trc.2024.104537.
- [17] Liang, Y., Liu, Y., Wang, X., Zhao, Z., 2024. Exploring large language models for human mobility prediction under public events. *Computers, Environment and Urban Systems* 112, 102153.
- [18] Liu, L., Chen, J., Wu, H., Zhen, J., Li, G., Lin, L., 2020. Physical-virtual collaboration modeling for intra- and inter-station metro ridership prediction. *IEEE Transactions on Intelligent Transportation Systems* 23, 3377–3391.
- [19] Liu, L., Zhu, Y., Li, G., Wu, Z., Bai, L., Mao, M., Lin, L., 2021. Online metro origin-destination prediction via heterogeneous information aggregation. *IEEE Transactions on Pattern Analysis and Machine Intelligence* 45, 3574–3589.
- [20] Liu, X., Lei, Z., Duan, Z., 2024. Assessing metro network vulnerability with turn-back operations: A monte carlo method. *Physica A: Statistical Mechanics and its Applications* .
- [21] Makhdomi, A.A., Gillani, I.A., 2023. Gnn-based passenger request prediction. *ArXiv abs/2301.02515*.
- [22] Masud, H., 2019. Travel behavior reactions to transit services disruptions: A case study on the washington d.c. metro safetrack project, in: 98th Annual Meeting of the Transportation Research Board.
- [23] Mo, B., Koutsopoulos, H.N., Zhao, J., 2022. Inferring passenger responses to urban rail disruptions using smart card data: A probabilistic framework. *Transportation Research Part E: Logistics and Transportation Review* .
- [24] Ni, M., He, Q., Gao, J., 2017. Forecasting the subway passenger flow under event occurrences with social media. *IEEE Transactions on Intelligent Transportation Systems* 18, 1623–1632.
- [25] Nian, G., Chen, F., Li, Z., Zhu, Y., Sun, D., 2019. Evaluating the alignment of new metro line considering network vulnerability with passenger ridership. *Transportmetrica A: Transport Science* 15, 1402 – 1418.
- [26] Noursalehi, P., Koutsopoulos, H.N., Zhao, J., 2018. Real time transit demand prediction capturing station interactions and impact of special events. *Transportation Research Part C: Emerging Technologies* 97, 277–300. doi:<https://doi.org/10.1016/j.trc.2018.10.023>.
- [27] Noursalehi, P., Koutsopoulos, H.N., Zhao, J., 2021. Dynamic origin-destination prediction in urban rail systems: A multi-resolution spatio-temporal deep learning approach. *IEEE Transactions on Intelligent Transportation Systems* 23, 5106–5115.

- [28] Pan, S., Ling, S., Jia, N., Liu, Y., He, Z., 2024. On the dynamic vulnerability of an urban rail transit system and the impact of human mobility. *Journal of Transport Geography* .
- [29] Paulsen, M., Rasmussen, T.K., Nielsen, O.A., . Modelling railway-induced passenger delays in multi-modal public transport networks: An agent-based copenhagen case study using empirical train delay data: 14th conference on advanced systems in public transport and TransitData 2018.
- [30] Qi, Q., Meng, Y., Zhao, X., Liu, J., 2022. Resilience assessment of an urban metro complex network: A case study of the zhengzhou metro. *Sustainability* .
- [31] Ronneberger, O., Fischer, P., Brox, T., 2015. U-net: Convolutional networks for biomedical image segmentation, in: *Medical image computing and computer-assisted intervention–MICCAI 2015: 18th international conference, Munich, Germany, October 5-9, 2015, proceedings, part III* 18, Springer. pp. 234–241.
- [32] Rubin, J., Brewin, C.R., Greenberg, N., Simpson, J., Wessely, S., 2005. Psychological and behavioural reactions to the bombings in london on 7 july 2005: cross sectional survey of a representative sample of londoners. *BMJ : British Medical Journal* 331, 606.
- [33] Scott, M., Su-In, L., et al., 2017. A unified approach to interpreting model predictions. *Advances in neural information processing systems* 30, 4765–4774.
- [34] Shen, Y., Ren, G., Ran, B., 2019. Cascading failure analysis and robustness optimization of metro networks based on coupled map lattices: a case study of nanjing, china. *Transportation* 48, 537 – 553.
- [35] da Silva, R.C., Kang, S.M., Airoidi, E.M., 2015. Predicting traffic volumes and estimating the effects of shocks in massive transportation systems. *Proceedings of the National Academy of Sciences* 112, 5643 – 5648.
- [36] Su, G., Si, B., Zhi, K., Zhao, B., Zheng, X., 2023. Simulation-based method for the calculation of passenger flow distribution in an urban rail transit network under interruption. *Urban Rail Transit* ,1–17.
- [37] Sun, H., Wu, J., Wu, L., Yan, X., Gao, Z., 2016. Estimating the influence of common disruptions on urban rail transit networks. *Transportation Research Part A-policy and Practice* 94, 62–75.
- [38] Sun, L., Huang, Y., Chen, Y., Yao, L., 2018. Vulnerability assessment of urban rail transit based on multi-static weighted method in beijing, china. *Transportation Research Part A-policy and Practice* 108, 12–24.
- [39] Tan, E., Ma, X., Du, Y., Zhang, Z., 2024. Enhancing urban metro system resilience under disruptive events through multi-agent reinforcement learning. *Journal of Transportation Safety & Security* .

- [40] Toque, F., Côme, É., Mahrsi, M.K.E., Oukhellou, L., 2016. Forecasting dynamic public transport origin-destination matrices with long-short term memory recurrent neural networks. 2016 IEEE 19th International Conference on Intelligent Transportation Systems (ITSC) , 1071–1076.
- [41] Wang, Y., Yin, H., Chen, H., Wo, T., Xu, J., Zheng, K., 2019. Origin-destination matrix prediction via graph convolution: a new perspective of passenger demand modeling. Proceedings of the 25th ACM SIGKDD International Conference on Knowledge Discovery & Data Mining .
- [42] yue Xu, X., Zhang, K., Mi, Z., Wang, X., 2023. Short-term passenger flow prediction during station closures in subway systems. Expert Syst. Appl. 236, 121362.
- [43] Xue, G., Liu, S., Ren, L., Ma, Y., Gong, D., 2021. Forecasting the subway passenger flow under event occurrences with multivariate disturbances. Expert Syst. Appl. 188, 116057.
- [44] Yap, M., Cats, O., 2020. Predicting disruptions and their passenger delay impacts for public transport stops. Transportation 48, 1703 – 1731.
- [45] Yap, M., Cats, O., Krasemann, J.T., van Oort, N., Hoogendoorn, S.P., 2021. Quantification and control of disruption propagation in multi-level public transport networks. International journal of transportation science and technology .
- [46] Ye, J., Zhao, J., Zheng, F., Xu, C., 2022. Completion and augmentation-based spatiotemporal deep learning approach for short-term metro origin-destination matrix prediction under limited observable data. Neural Computing and Applications 35, 3325–3341.
- [47] Zhang, J., Ren, G., Song, J., 2023a. Resilience-based optimization model for emergency bus bridging and dispatching in response to metro operational disruptions. PLOS ONE 18, 1–22. URL: <https://doi.org/10.1371/journal.pone.0277577>, doi:10.1371/journal.pone.0277577.
- [48] Zhang, J., Wang, S., Wang, X., 2018. Comparison analysis on vulnerability of metro networks based on complex network. Physica A-statistical Mechanics and Its Applications 496, 72–78.
- [49] Zhang, J., Xu, X., Hong, L., Wang, S., Fei, Q., 2011. Networked analysis of the shanghai subway network, in china. Physica A-statistical Mechanics and Its Applications 390, 4562–4570.
- [50] Zhang, J., Zheng, Y., Qi, D., 2017. Deep spatio-temporal residual networks for city-wide crowd flows prediction. Proceedings of the AAAI Conference on Artificial Intelligence 31. URL: <https://ojs.aaai.org/index.php/AAAI/article/view/10735>, doi:10.1609/aaai.v31i1.10735.
- [51] Zhang, N., Graham, D.J., Hörcher, D., Bansal, P., 2020. A causal inference approach to measure the vulnerability of urban metro systems. Transportation 48, 3269 – 3300.

- [52] Zhang, N., Horcher, D., Bansal, P., Graham, D.J., 2023b. Causal inference for disruption management in urban metro networks. [arXiv:2310.07514](https://arxiv.org/abs/2310.07514).
- [53] Zhu, G., Ding, J., Wei, Y., Yi, Y., Xu, S.S.D., Wu, E.Q., 2024. Two-stage od flow prediction for emergency in urban rail transit. *IEEE Transactions on Intelligent Transportation Systems* 25, 920–928. doi:10.1109/TITS.2023.3235413.
- [54] Zou, L., Wang, Z., Guo, R., 2024. Real-time prediction of transit origin–destination flows during underground incidents. *Transportation Research Part C: Emerging Technologies*.

Appendix A. Proof of Theorem 3.1

Theorem 3.1

If there are n samples obeying the linear model with noised samples in definition 3.1 and we fit a model with these samples, resulting in the fitted parameter $\hat{\beta}$. Then, the square distance between true parameter and the fitted parameter is bounded by:

$$E(\beta - \hat{\beta})^2 = (1 - p) |\beta|^2 + c \frac{(p\sigma_2^2 + \sigma_1^2)}{n}$$

Proof:

Suppose $X \in R^{n \times d}, Y \in R^n, \beta \in R^d$, where n is sample size and d is the dimension of feature. We first show that the l_2 loss can be decomposed to the summation of bias and variance of $\hat{\beta}$, then we tackle both bias and variance.

1) bias and variance decomposition:

$$\begin{aligned} E(\beta - \hat{\beta})^2 &= E(\beta - E\hat{\beta} + E\hat{\beta} - \hat{\beta})^2 \\ &= E(\beta - E\hat{\beta})^2 + E(E\hat{\beta} - \hat{\beta})^2 + 2E[(\beta - E\hat{\beta})(E\hat{\beta} - \hat{\beta})] \end{aligned}$$

Because $E[(\beta - E\hat{\beta})(E\hat{\beta} - \hat{\beta})] = (\beta - E\hat{\beta}) E(E\hat{\beta} - \hat{\beta}) = (\beta - E\hat{\beta}) \times (E\hat{\beta} - E\hat{\beta}) = 0$

Then:

$$E(\beta - \hat{\beta})^2 = E(\beta - E\hat{\beta})^2 + E(E\hat{\beta} - \hat{\beta})^2 = \text{bias}(\hat{\beta})^2 + \text{Tr}(\text{Var}(\hat{\beta}))$$

2) bias term:

$$E(\hat{\beta}) = E[(XX^T)^{-1} X^T Y] = (XX^T)^{-1} X^T E(Y|X)$$

Then:

$$E(Y|X) = (1 - p) \times E\epsilon_1 + pE(\epsilon_1 + (\beta^T X + \epsilon_2)) = pX\beta$$

Therefore:

$$E(\hat{\beta}) = E(1 - p) (XX^T)^{-1} X^T X\beta = p\beta$$

So:

$$\text{bias}(\hat{\beta})^2 = ((1-p)\beta)^2$$

3) variance term:

$$\text{Var}(\hat{\beta}) = \text{Var}\left((XX^T)^{-1}X^TY\right) = (XX^T)^{-1}X^T\text{Var}(Y|X)X(XX^T)^{-1}$$

Then:

$$\text{Var}(Y|X) = ((1-p)\sigma_1^2 + p(\sigma_1^2 + \sigma_2^2))I_n = (\sigma_1^2 + p\sigma_2^2)I_n$$

Where I_n is $n \times n$ identical matrix. Substituting it into $\text{Var}(\hat{\beta})$

$$\text{Var}(\hat{\beta}) = (XX^T)^{-1}X^T(\sigma_1^2 + p\sigma_2^2)I_nX(XX^T)^{-1}$$

Then:

$$\text{Tr}(\text{Var}(\hat{\beta})) = (\sigma_1^2 + p\sigma_2^2)\text{Tr}((XX^T)^{-1})$$

Suppose each entry in X is i.i.d sample from $N(0, \sigma_x^2)$, then XX^T is Wishart distribution [4] and:

$$E\text{Tr}(XX^T)^{-1} = \frac{d}{(n-d-1)\sigma_x^2}$$

Then:

$$\text{Tr}(\text{Var}(\hat{\beta})) = (\sigma_1^2 + p\sigma_2^2)\frac{d}{(n-d-1)\sigma_x^2}$$

For large n :

$$\text{Tr}(\text{Var}(\hat{\beta})) \approx (\sigma_1^2 + p\sigma_2^2)\frac{d}{n\sigma_x^2}$$

4) integrate two terms:

$$E(\beta - \hat{\beta})^2 = (1-p)^2\beta^2 + (\sigma_1^2 + p\sigma_2^2)\frac{d}{n\sigma_x^2} = (1-p)^2\beta^2 + c\frac{\sigma_1^2 + p\sigma_2^2}{n}$$

where:

$$c = \frac{d}{\sigma_x^2}$$

□

Appendix B. Proof of Theorem 3.2

We first elaborate this theorem in detail again.

Theorem 3.1

If the influence factors about the causal effects is noted as x , the causal effect is denoted as y , assume y and x obeys the following rule:

$$y = \epsilon_1 \text{ with probability } 1-p$$

$$y = \epsilon_1 + (f(x) + \epsilon_2) \text{ with probability } p$$

Where ϵ_1 following normal distribution $N(0, \sigma_1^2)$ and ϵ_2 following normal distribution $N(0, \sigma_2^2)$, β is the parameter and p is a constant between 0 and 1.

If we have observed a lot of (x_i, p_i) and a prediction model $\hat{y} = \hat{f}(x)$ And we have a threshold P , for each OD, if p_i , is greater than P , we will use causal effect prediction model to adjust it, otherwise we will just regard the prediction of normal model as the final prediction value. Then we can get the risk of this strategy.

$$E(y - \hat{y})^2 = \frac{1}{2}P^2(Ef(x)^2 + E\hat{f}(x)^2 - E(\hat{f}(x) - f(x))^2) - PE\hat{f}(x)^2 + c$$

proof:

There are 4 cases: the OD is truly affected, but we not adjust; the OD is truly affected and we adjust it; the OD is not truly affected, and we not adjust; the OD is not truly affected but we adjust it; We need add the risk of these four cases:

$$\begin{aligned} E(y - \hat{y})^2 &= E \int P(p_i > P \text{ and } y_i = \epsilon_1 + (f(x_i) + \epsilon_2)) \left(\hat{f}(x_i) - (\epsilon_1 + (f(x_i) + \epsilon_2)) \right)^2 dp_i \\ &+ \int P(p_i > P \text{ and } y_i = \epsilon_1) \left(\hat{f}(x_i) - \epsilon_1 \right)^2 dp_i \\ &+ \int P(p_i < P \text{ and } y_i = \epsilon_1) \epsilon_1^2 dp_i \\ &+ \int P(p_i < P \text{ and } y_i = \epsilon_1 + (f(x_i) + \epsilon_2)) (\epsilon_1 + (f(x_i) + \epsilon_2))^2 dp_i. \end{aligned}$$

The first term in the risk when the OD is affected and we adjust it, the second is the risk when the OD is not affected but we adjust it. Because $P(y_i = \epsilon_1 + (\beta^T x + \epsilon_2)) = p_i$ and $P(y_i = \epsilon_1) = 1 - p_i$, and we further need to assume p_i obey uniform distribution in $[0,1]$. then the above expression equals to:

$$\begin{aligned} E(y - \hat{y})^2 &= E \left[\int_P^1 t \left(\hat{f}(x) - (\epsilon_1 + (f(x) + \epsilon_2)) \right)^2 dt + \int_P^1 (1 - t) \left(\hat{f}(x) - \epsilon_1 \right)^2 dt \right. \\ &\left. + \int_0^P t (\epsilon_1 + (f(x) + \epsilon_2))^2 dt + \int_0^P (1 - t) \epsilon_1^2 dt \right]. \end{aligned}$$

Because ϵ_1 follows normal distribution $N(0, \sigma_1^2)$ and ϵ_2 follows normal distribution $N(0, \sigma_2^2)$ and we further assume they are independent. Therefore, we have:

$$Ef(x)\epsilon_1 = 0, \quad Ef(x)\epsilon_2 = 0, \quad E\epsilon_1\epsilon_2 = 0$$

Then by some calculation, we can get:

$$\begin{aligned} E(y - \hat{y})^2 &= \frac{1}{2}P^2 \left(Ef(x)^2 + E\hat{f}(x)^2 - E(\hat{f}(x) - f(x))^2 \right) \\ &- PE\hat{f}(x)^2 + E \left(\hat{f}(x)^2 + \frac{f(x)^2}{2} - f(x)\hat{f}(x) \right) + \sigma_1^2 + \frac{\sigma_2^2}{2} \\ &= \frac{1}{2}P^2 \left(Ef(x)^2 + E\hat{f}(x)^2 - E(\hat{f}(x) - f(x))^2 \right) - PE\hat{f}(x)^2 + c. \end{aligned}$$

where:

$$c = E \left(\hat{f}(x)^2 + \frac{f(x)^2}{2} - f(x) \hat{f}(x) \right) + \sigma_1^2 + \frac{\sigma_2^2}{2}$$

□